Corrections to Capillary flow

- slip at the wall - Mooney analysis
- entrance and exit effects - Bagley correction
- Non-parabolic velocity profile - Weissenberg-Rabinowitsch correction

---

Slip at the wall - Mooney analysis

Slip at the wall reduces the shear rate near the wall.

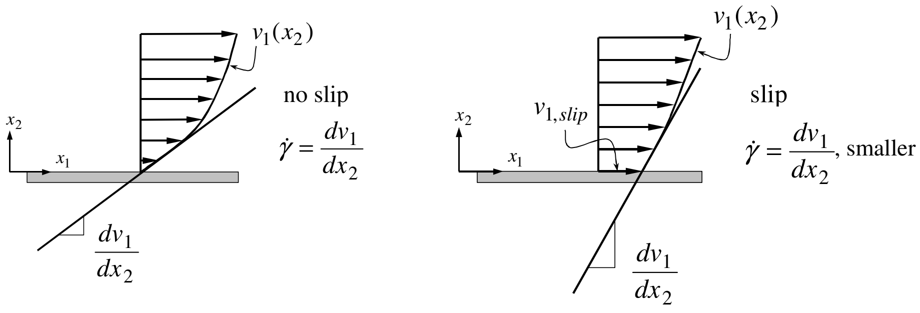

Slip at the wall - Mooney analysis

Slip at the wall reduces the shear rate near the wall.

$$\dot{\gamma}_{a,slip-corrected} \equiv \frac{4v_{z,av}}{R} - \frac{4v_{z,slip}}{R}$$

$$\frac{4v_{z,av}}{R} = \underbrace{4v_{z,slip}}_{\text{slope}}\left(\frac{1}{R}\right) + \underset{\text{intercept}}{\dot{\gamma}_{a,slip-corrected}}$$

$$\frac{4v_{z,av}}{R} = \frac{4Q_{measured}}{\pi R^3}$$

The Mooney correction is a correction to the apparent shear rate

Slip at the wall - **Mooney analysis**

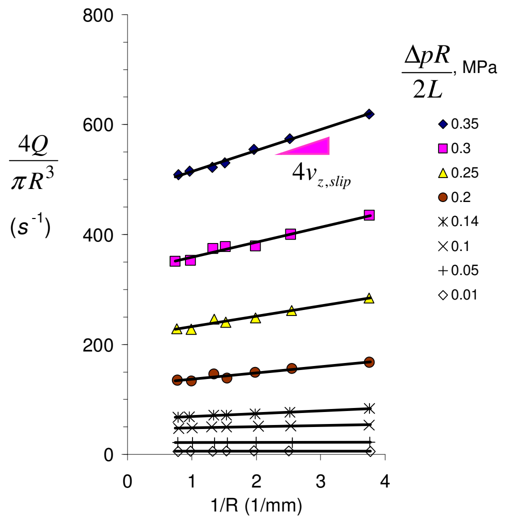

Figure 10.10, p. 396
Ramamurthy, LLDPE

Entrance and exit effects - Bagley correction

$$\tau_R = \frac{\Delta P R}{2L} \Rightarrow \quad \Delta P = (2\tau_R)\frac{L}{R}$$

Constant at constant Q

Run for different capillaries

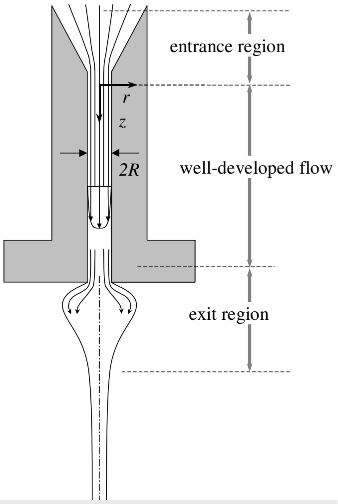

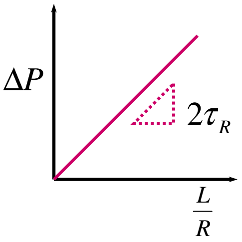

This is the result when the end effects are negligible.

The Bagley correction is a correction to the wall shear stress

---

Bagley Plot

$$\Delta P_{\substack{end\\effects}} = f(Q) = f(\dot{\gamma}_a)$$

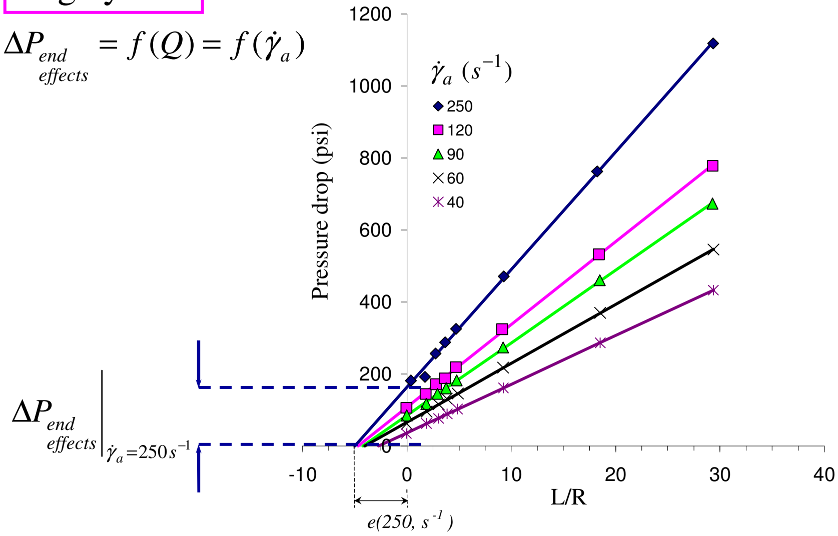

Figure 10.8, p. 394 Bagley, PE

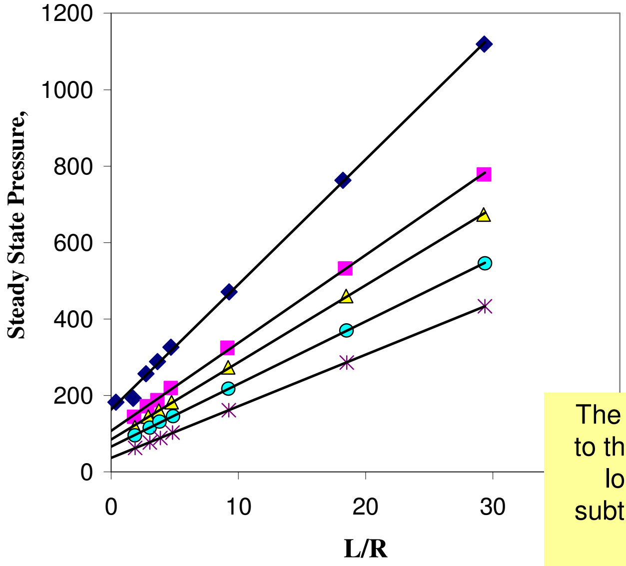

y = 32.705x + 163.53
$R^2 = 0.9987$
y = 22.98x + 107.72
$R^2 = 0.9997$
y = 20.172x + 85.311
$R^2 = 0.9998$
y = 16.371x + 66.018
$R^2 = 0.9998$
y = 13.502x + 36.81
$R^2 = 1$

The intercepts are equal to the entrance pressure losses; these must be subtracted from the data to get true pressure versus L/R.

Figure 10.8, p. 394 Bagley, PE

Figure 10.8, p. 394 Bagley, PE

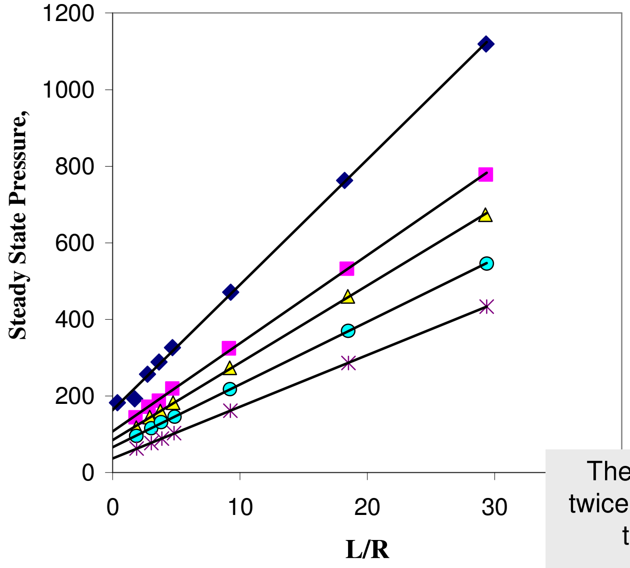

y = 32.705x + 163.53
$R^2 = 0.9987$
y = 22.98x + 107.72
$R^2 = 0.9997$
y = 20.172x + 85.311
$R^2 = 0.9998$
y = 16.371x + 66.018
$R^2 = 0.9998$
y = 13.502x + 36.81
$R^2 = 1$

The slopes are equal to twice the shear stress for the various apparent shear rates

$$\tau_{rz} = \frac{\Delta p R}{2L} \quad \Rightarrow \quad \Delta p = 2\tau_{rz}\left(\frac{L}{R}\right)$$

The data so far:

gammdotA (1/s)	deltPent psi	slope psi	sh stress psi	sh stress Pa
250	163.53	32.705	16.3525	1.1275E+05
120	107.72	22.98	11.49	7.9220E+04
90	85.311	20.172	10.086	6.9540E+04
60	66.018	16.371	8.1855	5.6437E+04
40	36.81	13.502	6.751	4.6546E+04

Now, correct shear rate for non-parabolic velocity profile.

Figure 10.8, p. 394 Bagley, PE

Weissenberg-Rabinowitsch correction

$$\dot{\gamma}_R(\tau_R) = \frac{4Q}{\pi R^3}\overbrace{\left[\frac{1}{4}\left(3+\frac{d\ln\dot{\gamma}_a}{d\ln\tau_R}\right)\right]}$$

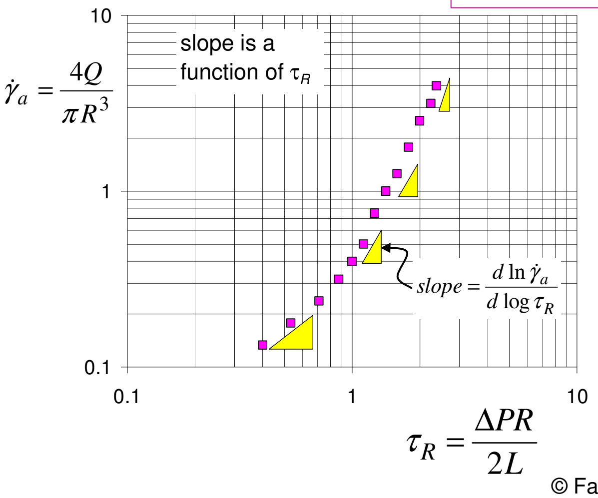

Sometimes the WR correction varies from point-to-point; sometimes it is a constant that applies to all data points.

Weissenberg-Rabinowitsch correction

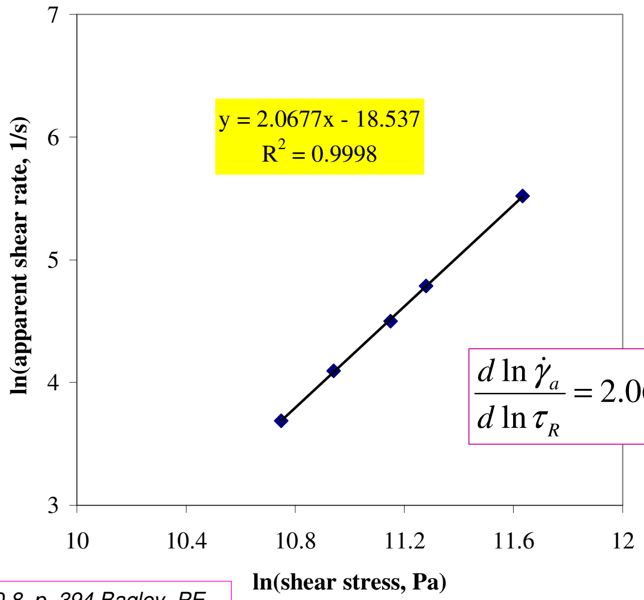

This slope is usually >1

$$\frac{d\ln\dot{\gamma}_a}{d\ln\tau_R} = 2.0677$$

Figure 10.8, p. 394 Bagley, PE

The data corrected for entrance/exit and non-parabolic velocity profile:

$$\eta = \frac{\tau_R}{\dot{\gamma}_R}$$

gammdotA (1/s)	deltPent psi	deltPent Pa	sh stress Pa	ln(sh st)	ln(gda)	WR correction	gam-dotR 1/s	viscosity Pa s
250	163.53	1.1275E+06	1.1275E+05	11.63289389	5.521460918	2.0677	316.73125	3.5597E+02
120	107.72	7.4270E+05	7.9220E+04	11.2799902	4.787491743	2.0677	152.031	5.2108E+02
90	85.311	5.8820E+05	6.9540E+04	11.14966143	4.49980967	2.0677	114.02325	6.0988E+02
60	66.018	4.5518E+05	5.6437E+04	10.9408774	4.094344562	2.0677	76.0155	7.4244E+02
40	36.81	2.5380E+05	4.6546E+04	10.74820375	3.688879454	2.0677	50.677	9.1849E+02

Now, plot viscosity versus wall-shear-rate

Figure 10.8, p. 394 Bagley, PE

Viscosity of polyethylene from Bagley's data

$$\eta = \frac{\tau_R}{\dot{\gamma}_R}$$

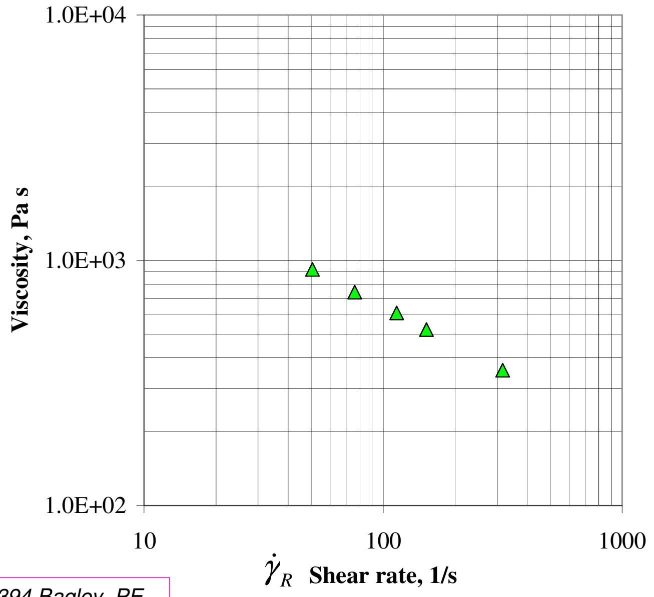

Figure 10.8, p. 394 Bagley, PE

© Faith A. Morrison, Michigan Tech U.

Viscosity from Capillary Experiments, Summary:

1. Take data of pressure-drop versus flow rate for capillaries of various lengths; perform Bagley correction (entrance pressure)
2. If possible, also take data for capillaries of different radii; perform Mooney correction (slip)
3. Perform the Weissenberg-Rabinowitsch correction (wall shear rate)
4. Plot true viscosity versus true wall shear rate

raw data: $\Delta P(Q)$

final data: $\eta = \tau_R / \dot{\gamma}_R$

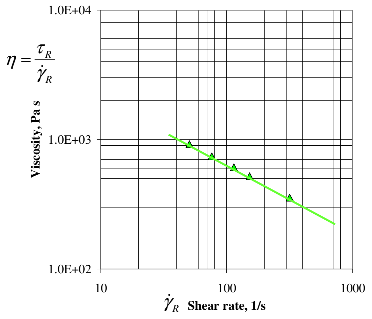

© Faith A. Morrison, Michigan Tech U.

Other Experimental Shear Geometries

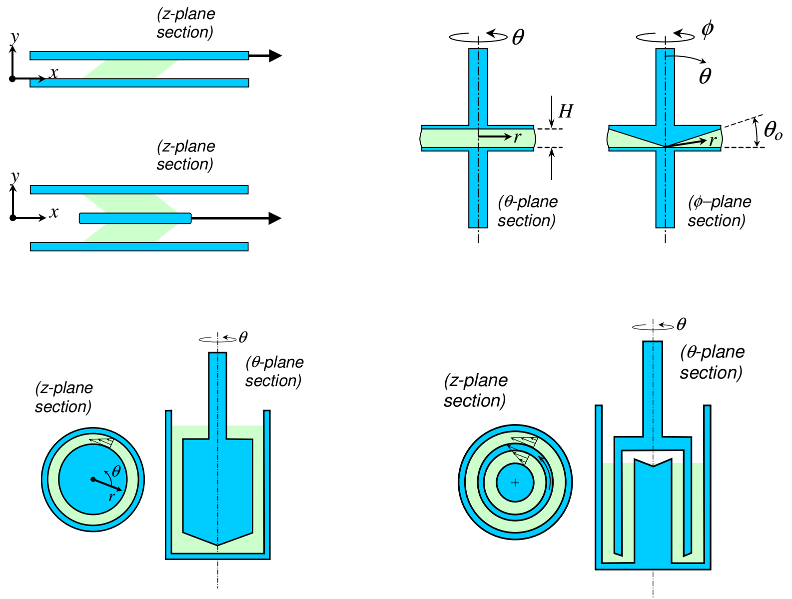

Why do we need more than one method of measuring viscosity?

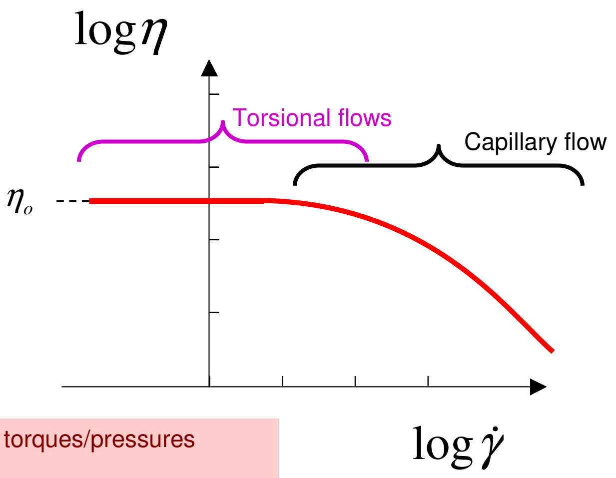

- At low rates, torques/pressures become low
- At high rates, torques/pressures become high; flow instabilities set in

Limits on Measurements: Flow instabilities in rheology

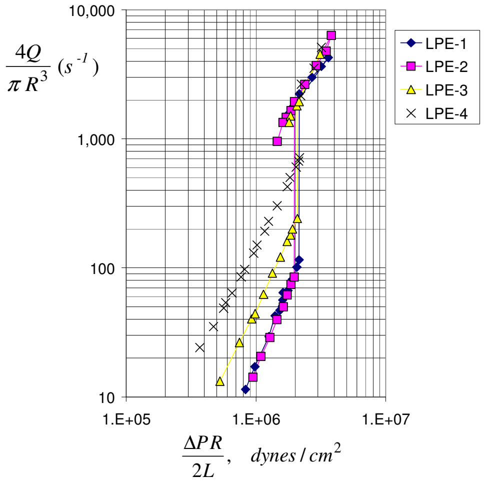

Figure 6.10, p. 177 Blyler and Hart; PE

capillary flow

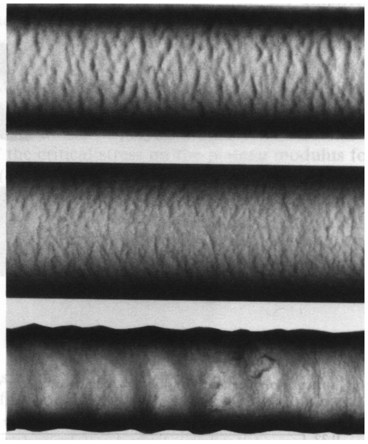

Figure 6.9, p. 176 Pomar et al. LLDPE

Torsional Parallel-Plate Flow - Viscosity

Measureables:
Torque **T** to turn plate
Rate of angular rotation **Ω**

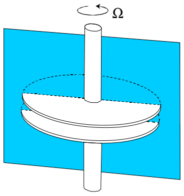

cross-sectional view:

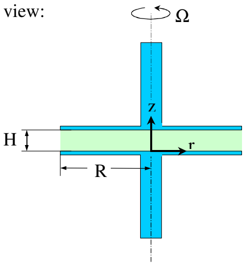

<u>Note:</u> shear rate experienced by fluid elements depends on their *r* position.

$$\dot{\gamma} = \frac{r\Omega}{H} = \dot{\gamma}_R \frac{r}{R}$$

By carrying out a Rabinowitsch-like calculation, we can obtain the stress at the rim (*r*=*R*).

$$\tau_{z\theta}\Big|_{r=R} = -T/2\pi R^3\left[3 + \frac{d\ln(T/2\pi R^3)}{d\ln\gamma_R}\right]$$

$$\boxed{\eta(\gamma_R) = \frac{-\tau_{z\theta}\big|_{r=R}}{\gamma_R}}$$

Correction required

Torsional Parallel-Plate Flow - correction

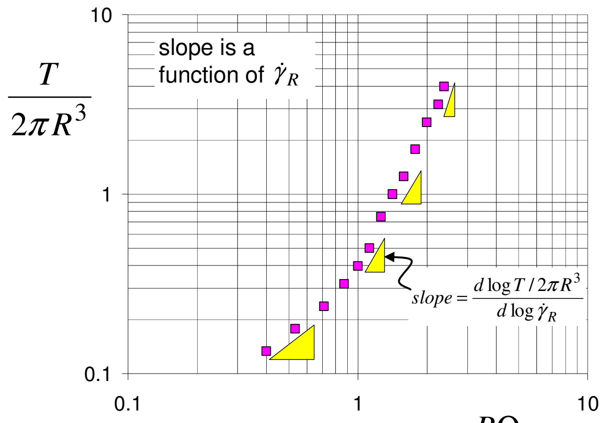

$$\dot{\gamma}_R = \frac{R\Omega}{H}$$

$$\boxed{\eta(\dot{\gamma}_R) = \frac{T/2\pi R^3}{\dot{\gamma}_R}\left[3 + \frac{d\ln(T/2\pi R^3)}{d\ln\dot{\gamma}_R}\right]}$$

© Faith A. Morrison, Michigan Tech U.

Torsional Cone-and-Plate Flow - Viscosity

Measureables:
Torque **T** to turn cone
Rate of angular rotation **Ω**

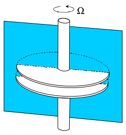

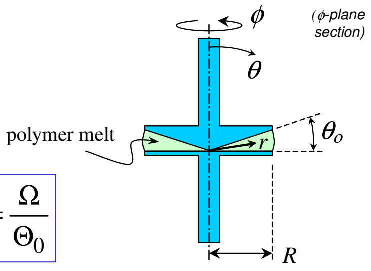

Note: the introduction of the cone means that shear rate is independent of *r*.

$$\boxed{\dot{\gamma} = \frac{\Omega}{\Theta_0}}$$

Since shear rate is constant everywhere, so is stress, and we can calculate stress from torque.

$$\boxed{\tau_{\theta\phi} = \text{constant} = \frac{3T}{2\pi R^3}}$$

$$\boxed{\eta(\dot{\gamma}) = \frac{3T\Theta_0}{2\pi R^3\Omega}}$$

No corrections needed in cone-and-plate

© Faith A. Morrison, Michigan Tech U.

Torsional Cone-and-Plate Flow – 1st Normal Stress

Measureables:
Normal thrust **F**

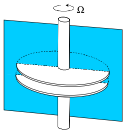

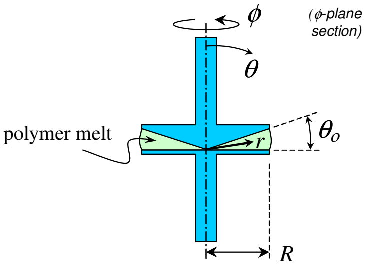

The total upward thrust of the cone can be related directly to the first normal stress coefficient.

$$F = \left[2\pi \int_0^R \Pi_{\theta\theta}\Big|_{\theta=\frac{\pi}{2}} r\,dr \right] - \pi R^2 p_{atm}$$

(see text pp404-5; also DPL pp522-523)

$$\boxed{\Psi_1(\dot{\gamma}) = \frac{2F\Theta_0^2}{\pi R^2 \Omega^2}}$$

Torsional Cone-and-Plate Flow – 2nd Normal Stress

- Cone and Plate:

$$\Pi_{22} - p_0 = -(N_1 + 2N_2)\ln\left(\frac{r}{R}\right) - N_2$$

Need normal force as a function of *r* / R

(see Bird et al., DPL)

- MEMS used to manufacture sensors at different radial positions

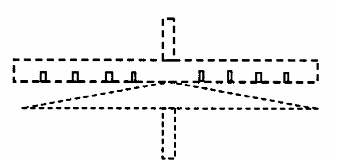

S. G. Baek and J. J. Magda, J. Rheology, 47(5), 1249-1260 (2003)

J. Magda et al. Proc. XIV International Congress on Rheology, Seoul, 2004.

RheoSense Incorporated (www.rheosense.com)

RheoSense Incorporated

Comparison with other instruments

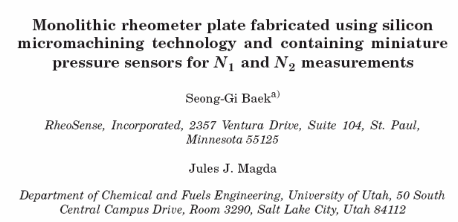

Monolithic rheometer plate fabricated using silicon micromachining technology and containing miniature pressure sensors for N_1 and N_2 measurements

Seong-Gi Baek[a)]

RheoSense, Incorporated, 2357 Ventura Drive, Suite 104, St. Paul, Minnesota 55125

Jules J. Magda

Department of Chemical and Fuels Engineering, University of Utah, 50 South Central Campus Drive, Room 3290, Salt Lake City, Utah 84112

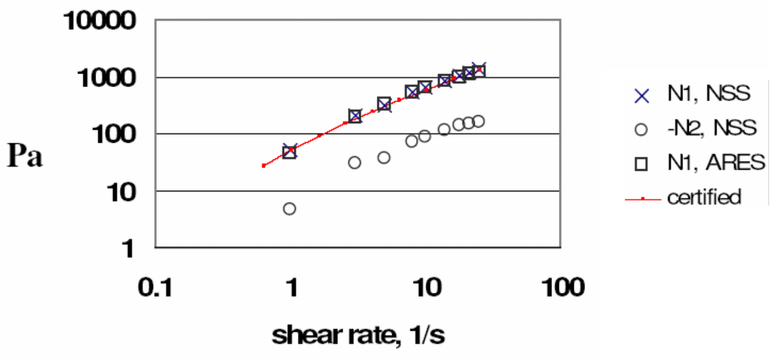

S. G. Baek and J. J. Magda, J. Rheology, 47(5), 1249-1260 (2003)

Limits on Measurements: Flow instabilities in rheology

cone and plate flow

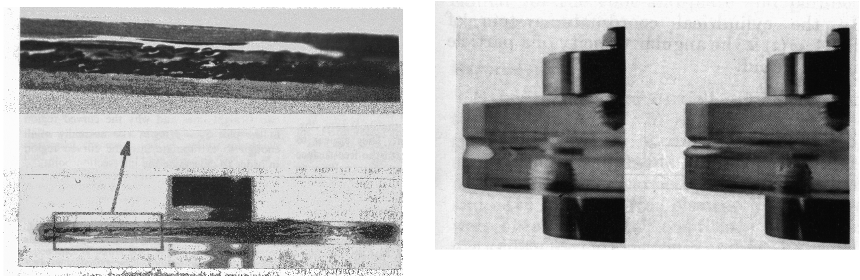

Figures 6.7 and 6.8, p. 175 Hutton; PDMS

Couette Flow

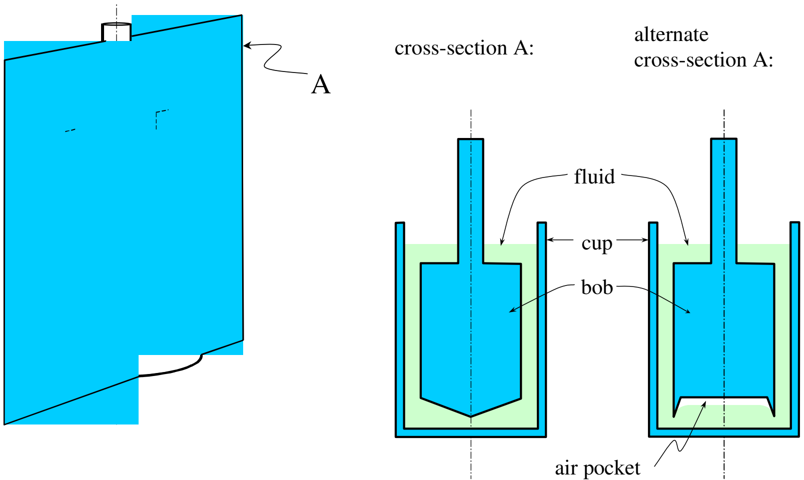

- see text
- useful for low viscosity fluids

Elongational Flow Measurements

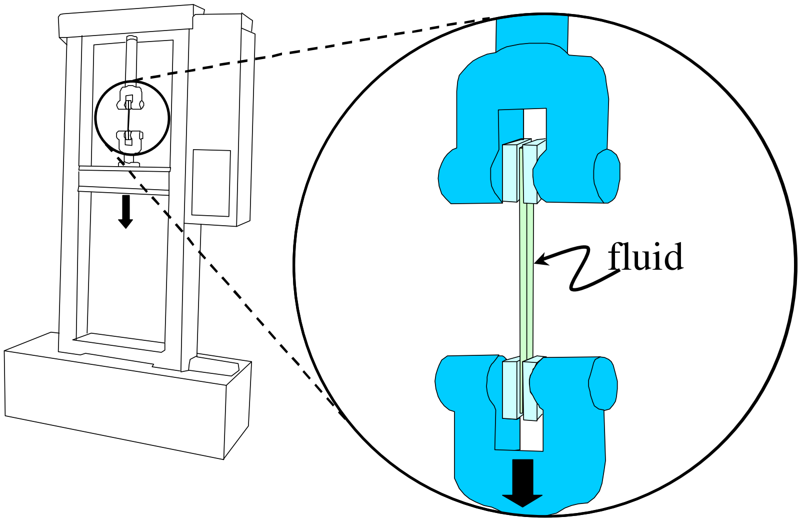

Experimental Elongational Geometries

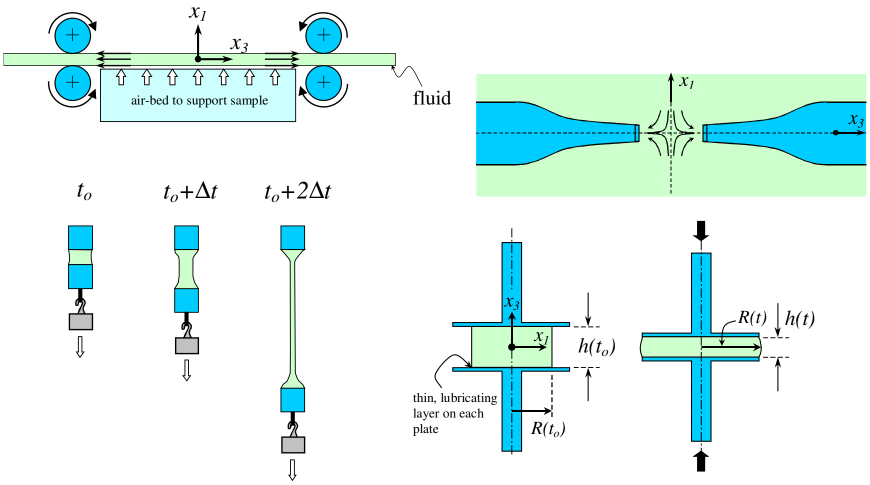

Uniaxial Extension

tensile force

$$\tau_{zz} - \tau_{rr} = -\frac{f(t)}{A(t)}$$

time-dependent cross-sectional area

For homogeneous flow: $A(t) = A_0 e^{-\varepsilon_0 t}$

$$\bar{\eta} = \frac{-(\tau_{zz} - \tau_{rr})}{\varepsilon_0} = \frac{f(t_\infty) e^{\varepsilon_0 t_\infty}}{A_0 \varepsilon_0}$$

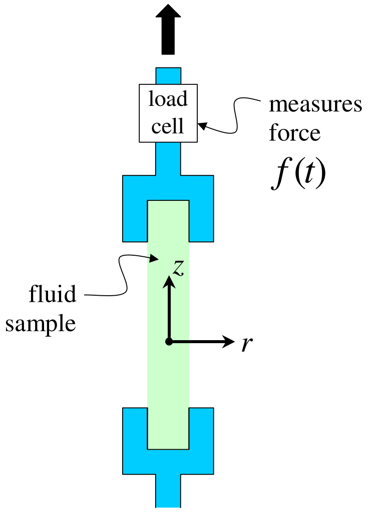

Experimental Difficulties in Elongational Flow

ideal elongational deformation

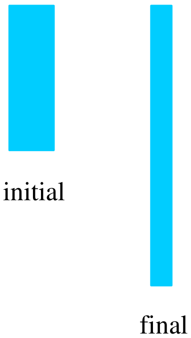

initial

final

experimental challenges

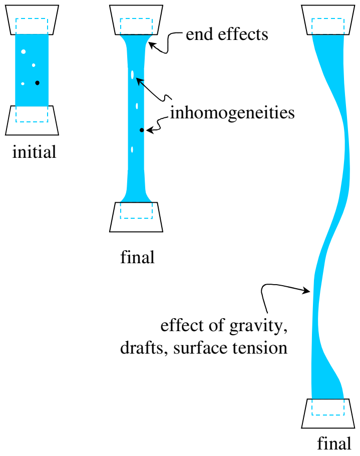

initial

end effects

inhomogeneities

final

effect of gravity, drafts, surface tension

final

Filament Stretching Rheometer (FiSER)

Tirtaatmadja and Sridhar, J. Rheol., 37, 1081-1102 (1993)

- •Optically monitor the midpoint size
- •Very susceptible to environment
- •End Effects

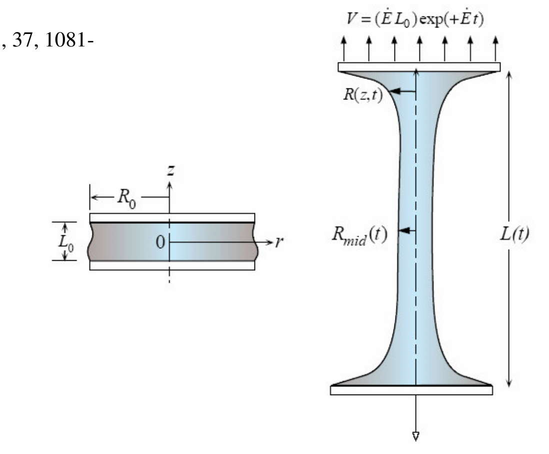

McKinley, et al., 15th Annual Meeting of the International Polymer Processing Society, June 1999.

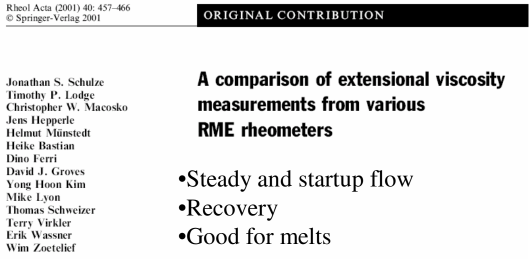

Rheol Acta (2001) 40: 457–466
© Springer-Verlag 2001

ORIGINAL CONTRIBUTION

Jonathan S. Schulze
Timothy P. Lodge
Christopher W. Macosko
Jens Hepperle
Helmut Münstedt
Heike Bastian
Dino Ferri
David J. Groves
Yong Hoon Kim
Mike Lyon
Thomas Schweizer
Terry Virkler
Erik Wassner
Wim Zoetelief

A comparison of extensional viscosity measurements from various RME rheometers

- Steady and startup flow
- Recovery
- Good for melts

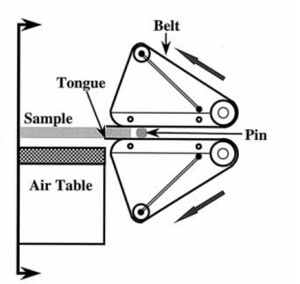

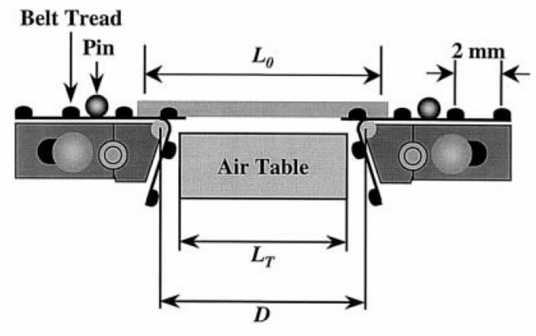

RHEOMETRICS RME

© Faith A. Morrison, Michigan Tech U.

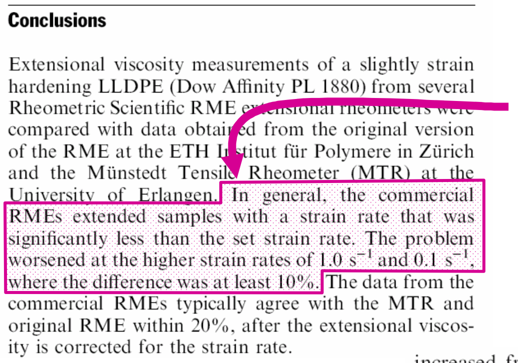

Conclusions

Extensional viscosity measurements of a slightly strain hardening LLDPE (Dow Affinity PL 1880) from several Rheometric Scientific RME extensional rheometers were compared with data obtained from the original version of the RME at the ETH Institut für Polymere in Zürich and the Münstedt Tensile Rheometer (MTR) at the University of Erlangen. In general, the commercial RMEs extended samples with a strain rate that was significantly less than the set strain rate. The problem worsened at the higher strain rates of 1.0 s^{-1} and 0.1 s^{-1}, where the difference was at least 10%. The data from the commercial RMEs typically agree with the MTR and original RME within 20%, after the extensional viscosity is corrected for the strain rate.

Achieving commanded strain requires great care.

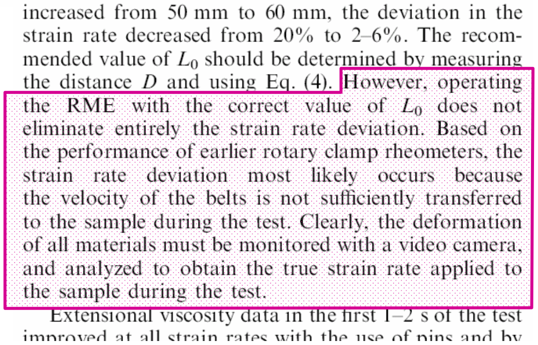

increased from 50 mm to 60 mm, the deviation in the strain rate decreased from 20% to 2–6%. The recommended value of L_0 should be determined by measuring the distance D and using Eq. (4). However, operating the RME with the correct value of L_0 does not eliminate entirely the strain rate deviation. Based on the performance of earlier rotary clamp rheometers, the strain rate deviation most likely occurs because the velocity of the belts is not sufficiently transferred to the sample during the test. Clearly, the deformation of all materials must be monitored with a video camera, and analyzed to obtain the true strain rate applied to the sample during the test.

Extensional viscosity data in the first 1–2 s of the test improved at all strain rates with the use of pins and by

Use of the video camera (although tedious) is recommended in order to get correct strain rate.

Sentmanat Extension Rheometer

- Originally developed for rubbers, good for melts
- Measures elongational viscosity, startup, other material functions
- Two counter-rotating drums
- Easy to load; reproducible

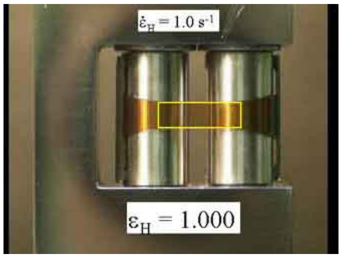

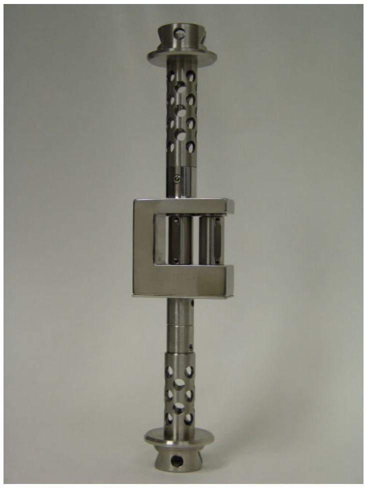

www.xpansioninstruments.com

© Faith A. Morrison, Michigan Tech U.

Sentmanat et al., J. Rheol., 49(3) 585 (2005)

Comparison on different host instruments

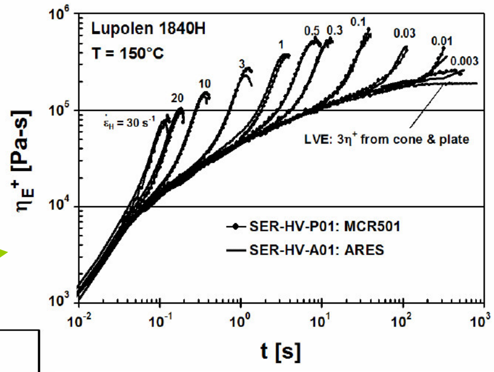

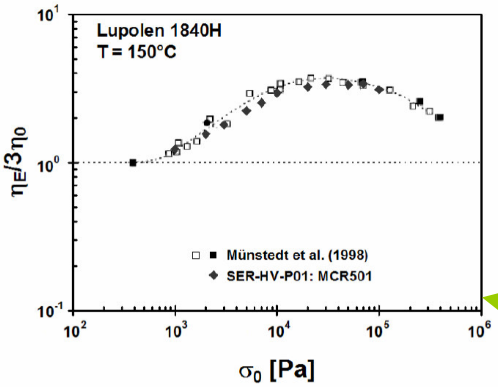

Comparison with other instruments (literature)

© Faith A. Morrison, Michigan Tech U.

CaBER Extensional Rheometer

- Polymer solutions
- Works on the principle of capillary filament break up
- Cambridge Polymer Group and HAAKE

For more on theory see: campoly.com/notes/007.pdf

Brochure: www.thermo.com/com/cda/product/detail/1,,17848,00.html

Operation

- Impose a rapid step elongation
- form a fluid filament, which continues to deform
- flow driven by surface tension
- also affected by viscosity, elasticity, and mass transfer
- measure midpoint diameter as a function of time
- Use force balance on filament to back out an apparent elongational viscosity

---

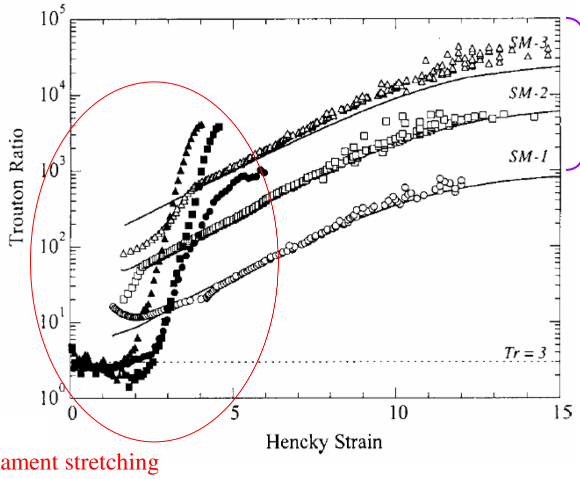

Capillary breakup experiments

Filament stretching apparatus

Comments

- Must know surface tension
- Transient agreement is poor
- Steady state agreement is acceptable
- Be aware of effect modeling assumptions on reported results

Anna and McKinley, *J. Rheol.* 45, 115 (2001).

Elongational Viscosity via Contraction Flow: Cogswell/Binding Analysis

Fluid elements along the centerline undergo considerable elongational flow

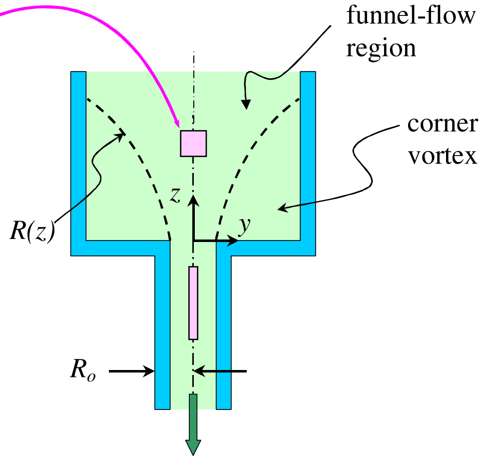

By making strong assumptions about the flow we can relate the pressure drop across the contraction to an elongational viscosity

---

Assumptions for the Cogswell Analysis

- incompressible fluid
- funnel-shaped flow; no-slip on funnel surface
- unidirectional flow in the funnel region
- well developed flow upstream and downstream
- θ-symmetry
- pressure drops due to shear and elongation may be calculated separately and summed to give the total entrance pressure-loss
- neglect Weissenberg-Rabinowitsch correction
- shear stress is related to shear-rate through a power-law
- elongational viscosity is constant
- shape of the funnel is determined by the minimum generated pressure drop
- no effect of elasticity (shear normal stresses neglected)
- neglect inertia

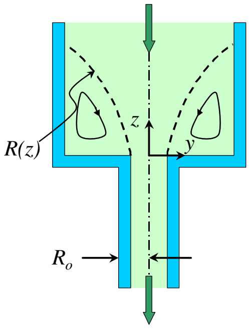

$$\dot{\gamma} \approx \dot{\gamma}_a$$

$$\tau_R = m\dot{\gamma}_a^n$$

$$\bar{\eta} = \text{constant}$$

F. N. Cogswell, Polym. Eng. Sci. (1972) 12, 64-73.
F. N. Cogswell, Trans. Soc. Rheol. (1972) 16, 383-403.

Cogswell Analysis

elongation rate
$$\dot{\varepsilon}_o = \frac{\tau_R \dot{\gamma}_a}{2(\tau_{11} - \tau_{22})}$$

$$\tau_R = \eta\,\dot{\gamma}_a$$

$$\dot{\gamma}_a = \frac{4Q}{\pi R^3}$$

$$\eta = m\dot{\gamma}_a^{n-1}$$

elongation normal stress
$$(\tau_{11} - \tau_{22}) = -\frac{3}{8}\Delta p_{ent} \quad (n+1)$$

elongation viscosity
$$\overline{\eta} \approx \frac{-(\tau_{11} - \tau_{22})}{\dot{\varepsilon}_o} = \frac{\frac{9}{32}(n+1)^2 \Delta p_{ent}^2}{\tau_R \dot{\gamma}_a}$$

Assumptions for the Binding Analysis

- incompressible fluid
- funnel-shaped flow; no-slip on funnel surface
- unidirectional flow in the funnel region
- well developed flow upstream and downstream
- θ -symmetry
- shear viscosity is related to shear-rate through a power-law
- elongational viscosity is given by a power law
- shape of the funnel is determined by the minimum work to drive flow
- no effect of elasticity (shear normal stresses neglected)
- the quantities $(dR/dz)^2$ and d^2R/dz^2, related to the shape of the funnel, are neglected; implies that the radial velocity is neglected when calculating the rate of deformation
- neglect energy required to maintain the corner circulation
- neglect inertia

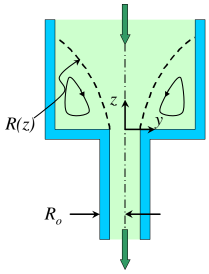

$$\tau_R = m\dot{\gamma}_a^n$$

$$\overline{\eta} = l\dot{\varepsilon}_o^{\,t-1}$$

D. M. Binding, JNNFM (1988) 27, 173-189.

Binding Analysis

l, elongational prefactor

$$\boxed{\Delta p_{ent}} = \frac{2m(1+t)^2}{3t^2(1+n)^2}\left\{\frac{lt(3n+1)n^t I_{nt}}{m}\right\}^{1/(1+t)} \dot{\gamma}_{R_o}{}^{t(n+1)/(1+t)}\left\{1-\alpha^{3t(n+1)/(1+t)}\right\}$$

$$I_{nt} = \int_0^1 \left|2-\left(\frac{3n+1}{n}\right)\phi^{1+1/n}\right|^{t+1}\phi\, d\phi$$

$$\boxed{\eta = m\dot{\gamma}_a^{n-1}}$$

$$\dot{\gamma}_{R_o} = \frac{(3n+1)\boxed{Q}}{n\pi R_o^3}$$

elongation viscosity $\eta = l\dot{\varepsilon}_o^{t-1}$

Rheotens (Goettfert)

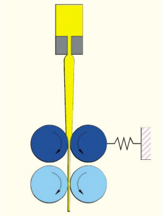

from their brochure:

"Rheotens test is a rather complicated function of the characteristics of the polymer, dimensions of the capillary, length of the spin line and of the extrusion history"

www.goettfert.com/downloads/Rheotens_eng.pdf

- Does not measure material functions without constitutive model
- small changes in material properties are reflected in curves
- easy to use
- excellent reproducibility
- models fiber spinning, film casting
- widespread application

An elongational viscosity may be extracted from a “grand master curve” under some conditions

"The rheology of the rheotens test,“ M.H. Wagner, A. Bernnat, and V. Schulze, J. Rheol. 42, 917 (1998)

Raw data

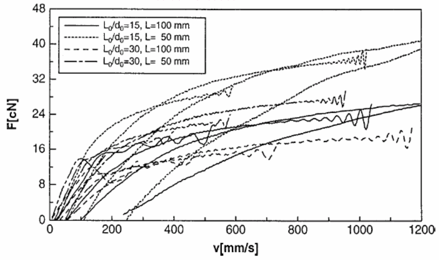

Grand master curve

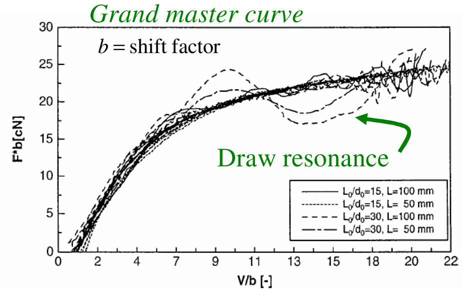

b = shift factor

Draw resonance

vs. draw ratio $V = v/v_{\text{die exit}}$

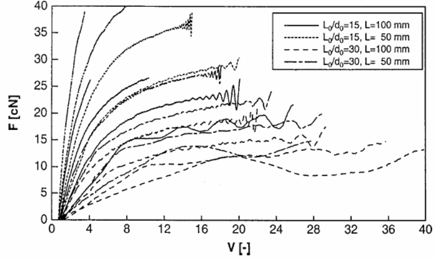

Summary

SHEAR

- •Shear measurements are readily made
- •Choice of shear geometry is driven by fluid properties, shear rates
- •Care must be taken with automated instruments (nonlinear response, instrument inertia, resonance, motor dynamics)

ELONGATION

- •Elongational properties are still not routine
- •Newer instruments (RME, Sentmanat,CaBER) have improved the possibility of routine elongational flow measurements
- •Some measurements are best left to the researchers dedicated to them due to complexity (FiSER)
- •Industries that rely on elongational flow properties (fiber spinning, foods) have developed their own ranking tests